Comparison of chemical and interpretative methods: the carbon-boron π-bond as a test case

Radhika Gupta,[a] Elixabete Rezabal,[a,b] Golshid Hasrack,[a] Camille Noûs,[c] Gilles Frison*,[a]

[a] LCM, CNRS, Ecole polytechnique, Institut Polytechnique de Paris, 91128 Palaiseau, France
[b] Faculty of Chemistry, University of the Basque Country UPV/EHU, Donostia International Physics Center (DIPC), 20018 Donostia, Spain
[c] Cogitamus Laboratory

Abstract

Quantum chemical calculations using DFT and NBO, ETS-NOCV, QTAIM and ELF interpretative approaches have been carried out on **X**-BH_2^+ borenium complexes for 39 divalent C-donor ligands **X** including various N-heterocyclic carbenes and carbones. The C-B bond length and the barrier of rotation around the C-B bond were calculated and compared with various descriptors of the C-B π-bond strength obtained from the orbital localization, energy partitioning or topological methods. Two families of descriptors emerged: *intrinsic* indicators, which measure the intensity of the π-bond in the investigated molecule, and *relative* indicators, among them the rotational barrier, which compare the studied molecule with its conformer in which the π-interaction is prevented. *Relative* indicators are influenced by other interactions in addition to purely π-interactions. For both families of descriptors, excellent correlations are obtained, showing that the interpretative methods, despite their conceptual differences, describe the same chemical properties. These results also reveal noticeable shortcomings in these methods, and some precautions that need to be taken to interpret their results adequately.

Author contributions

C.N., scientific consortium (http://www.cogitamus.fr/indexen.html) created to affirm the collaborative and open nature of knowledge creation and dissemination, contributed to the development of the methodological framework and the state of the research, all of which are effectively part of the collegial construction of the standards of science; E.R. and G.F. conceived the original idea; G.F. designed the study; R.G., E.R. and G.H performed the calculations; G.F. and R.G. analyzed and interpreted the results, with initial help from E.R.; G.F. wrote the manuscript with help from R.G and critical feedback from E.R. and G.H.

Introduction

Chemical bonds, among other "fuzzy" chemical concepts,[1,2] are not univocally defined and their quantification is not straightforward because they are not a quantum mechanical observable. However, chemical bonding is a key concept in chemistry, a cornerstone of this science.[3,4] In that context, numerous approaches have been developed in order to describe, classify and measure chemical bond. Experimentally, it is difficult to quantify a chemical bond, even if widely known indicators exist. The bond length, which from the chemist's point of view should be approximately correlated to its strength, can indeed be empirically related to a bond index[5] or compared to the sum of the covalent radii of the atoms involved.[6] The activation barrier associated to the rotation around the bond allows to differentiate a single bond (free rotation) from a double bond (strong rotation barrier).

The advent of theoretical and computational chemistry has made it possible to have straightforward access to these parameters by calculation, and simultaneously has led to the development of methods for bond analysis. These methods use different approaches to describe the molecular system under study.[7] A first representation can be made from the molecular orbitals used to describe the wave function. The bond order for π-bond in the Hückel framework defined by Coulson,[8] the Wiberg Bond Index (WBI)[9] and the Mayer bond order[10] are prominent examples derived from this approach.[11] Bonding analysis can also result from different procedures leading to localized molecular orbitals[12-14] or natural orbitals,[15] leading to methods such as the Localized orbital bonding analysis (LOBA) method[16,17] and the well-known natural bonding orbital (NBO) method.[18]

A second group of methods is based on the real-space partition of the molecular space using various functions such as the electronic density, the Pauli kinetic energy density, the reduced density gradient or the single-Exponential decay detector. These functions are used in the Bader's Quantum theory of atoms in molecules (QTAIM) method,[19] the electron localization function (ELF) method,[20,21] the non-covalent interaction (NCI) index[22] and the density overlap regions indicator (DORI) analysis,[23] respectively. An interesting picture of the chemical bond can also be obtained through the variations in isotropic magnetic shielding around a molecule,[24] or with the charge displacement analysis method.[25]

Chemical bond analysis can also be performed using energy decomposition approaches, such as the extended transition state (ETS)[26,27] or the energy decomposition analysis (EDA)[28] methods, possibly combined with the natural orbitals for chemical valence (NOCV) theory,[29] and the symmetry-adapted perturbation theory (SAPT) scheme.[30]

Finally, although force constants are known not to properly match the bond strengths,[31] derived methods such as the concept of adiabatic internal vibrational modes,[32] or the local stretching force[33] and compliance constants[34] also provide noteworthy chemical bond descriptors.

These many interpretative methods are widely used in the literature to provide insights into the nature of chemical bonds.[35-43] However, this plethora of methods, while of value in providing complementary visions of the same subject,[44-46] is also troublesome, in the sense that contradictory descriptions can result, leading to many controversies in the literature, whether it is to describe for example alkaline earth-[47-49] or metal-ligand bonds,[50,51] multiple bonds[52-54] weak bonds,[55-61] or rotational barrier of single bond.[62,63] In many cases too, there is no significant discrepancy between two different approaches, but the agreement is far from perfect. A noteworthy example is given in a recent study in which the internal π-donation to the carbene center within 15 *N*-heterocyclic carbenes (NHC) has been estimated through NBO and ETS-NOCV approaches.[64] Despite the

relevance of the two selected descriptors, the coefficient of determination (R^2) is not more than 0.89. If such computational approach is a powerful tool to qualitatively predict the trend comparing chemically similar systems, it raises questions about the reasons for the observed differences.

Depending on the theoretical model used, the numerical differences between several bond descriptors may result from many factors, such as the comparison of descriptors which might not be related to the same chemical concept, the misuse of methods, the misinterpretation of the results or the existence of conceptual problems in the definition of the descriptors. It is currently difficult to distinguish between these different assumptions and opinions may differ,[65,66] even if numerous efforts have been made to compare various methods, to analyze their differences and to propose unified approaches.[67-70]

The ability to establish cross correlations (or lack of correlations) between different approaches would, however, provide a better knowledge of the nature of the calculated descriptors, of the chemical concept under investigation, and could help in the development of future interpretative methods. In this context, the focus of the present work lies on the modeling, through various theoretical approaches, of the π-interaction between neutral divalent carbon-donor compounds and cationic BH_2^+ moiety. Borenium cations R_2BL^+ are well-known boron Lewis acids.[71] These boron species have been used in numerous catalytic processes.[72-75] They are stabilized through electronic π-donation from the π-cloud of the boron substituents,[76-79] and neutral divalent carbon-donor compounds, such as normal NHC,[80-85] mesoionic NHC[86] and carbones,[87] have been used for this purpose (Scheme 1). For dihydrido borenium (R = H), only their two-electrons σ-donor L ligand provide partial mitigation of their electron deficiency and their stabilization requires strong π-donor.[88,89] DFT studies on C-donor ligand-BR_2^+ borenium reveal a short CB bond reflecting a partial double-bond character due to C→B π-electronic transfer.[82,84,87-91] Beyond structural parameters, various theoretical indicators have been used to analyze the electronic structure of these and other related compounds,[92-94] among them the nature of the highest occupied and lowest unoccupied molecular orbitals (HOMO/LUMO), the atomic charges, the energy associated to the σ- and π-donation through energy decomposition analysis of the B-C bond, and the Wiberg bond index between these two atoms. Only few studies have used such indicators to compare the bonding situation in borenium complexes. The comparison of the bonding in various complexes between carbones $(PPh_3)_2C$ and EH_2^q (E^q = Be, B^+, C^{2+}, N^{3+}, O^{4+}) has been performed with the ETS-NOCV approach.[90] Recently, a combination of energy decomposition analysis methods has been used to clarify the theoretical measurement of the π-interactions strength within main group-NHC complexes, including NHC-borenium complexes.[95] Based on these previous studies, C-donor ligand - dihydrido borenium complexes, in which the π-interaction between the two fragments is limited to the C→B π-donation, appear as ideal models to assess the relevance of π-bond descriptors.

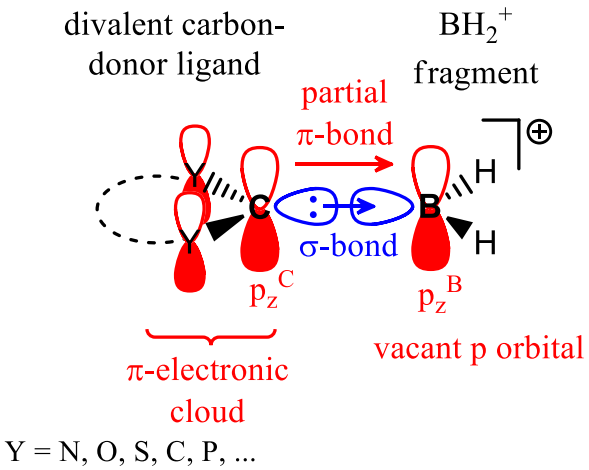

Scheme 1. Schematic description of the σ- and π-interaction in carbene and related compounds – BH_2^+ complexes

Result and discussion

Geometrical structures

39 divalent carbon compounds, including normal NHC (**1**-**2**, **4**, **6**, **8**, **10**, **12**, **14**, **16**, **20**-**24**, **26**-**28**, **30**-**33**), mesoionic NHC (**9**, **11**, **13**, **15**, **17**-**19**, **25**, **29**), cyclic alkyl amino carbenes (cAAC **3**, **5**, **7**), carbodiphosphoranes (**35**-**36**) and carbodicarbenes (**34**, **37**-**39**), have been selected, so as to ensure a wide variety of geometrical structures and electronic properties (Scheme 2).[96-99] Most of them, but **5**, **7**, **17**, **23**-**24**, **26**-**28** and **32**, are unsubstituted or "parent" molecules, preventing steric interference in the electronic analysis of their BH_2^+ complexes. The divalent carbon atom of **1**-**39** is linked to two atoms, noted Y, and possesses a lone pair located in the Y-C-Y plane. **1**-**39** bind to the BH_2^+ moiety to form the borenium cations **X**-BH_2^+ (**X** = **1**-**39**). Geometry optimization of **X**-BH_2^+ (**X** = **1**-**39**) at the DFT B3LYP/TZVP level leads to minimum on the potential energy surface for which the BH_2 and Y_2C moiety are coplanar or almost coplanar,[100] except for **3**, **5** and **7** (vide infra). This planar conformation will be noted hereafter as $\mathbf{X}^{//}$-BH_2^+. In addition to the σ-B-C bond formed by the donation of the in-plane lone pair of the carbon atom to the vacant sp^2-orbital of the boron atom (Scheme 1), this planarity supports the existence of a partial π-bond, the strength of which is supposed to depend on the nature of the π-system of the divalent donor ligand. The $\mathbf{X}^{//}$-BH_2^+ conformation of **X**-BH_2^+ (**X** = **3**, **5**, **7**) is a transition state for the rotation around the C-B bond, whereas the BH_2 and Y_2C moiety are perpendicular (Y-C-B-H dihedral angle around 90°) in the ground state. This conformation is noted as $\mathbf{X}^{\perp}$-BH_2^+ in the following. This result suggests weak π-donation capability for **3**, **5** and **7**. Furthermore, in addition to σ- and π-donations, it is likely that there are other weak electronic or steric interactions between the BH_2 and the C-donor ligand in the **X**-BH_2^+ complexes.

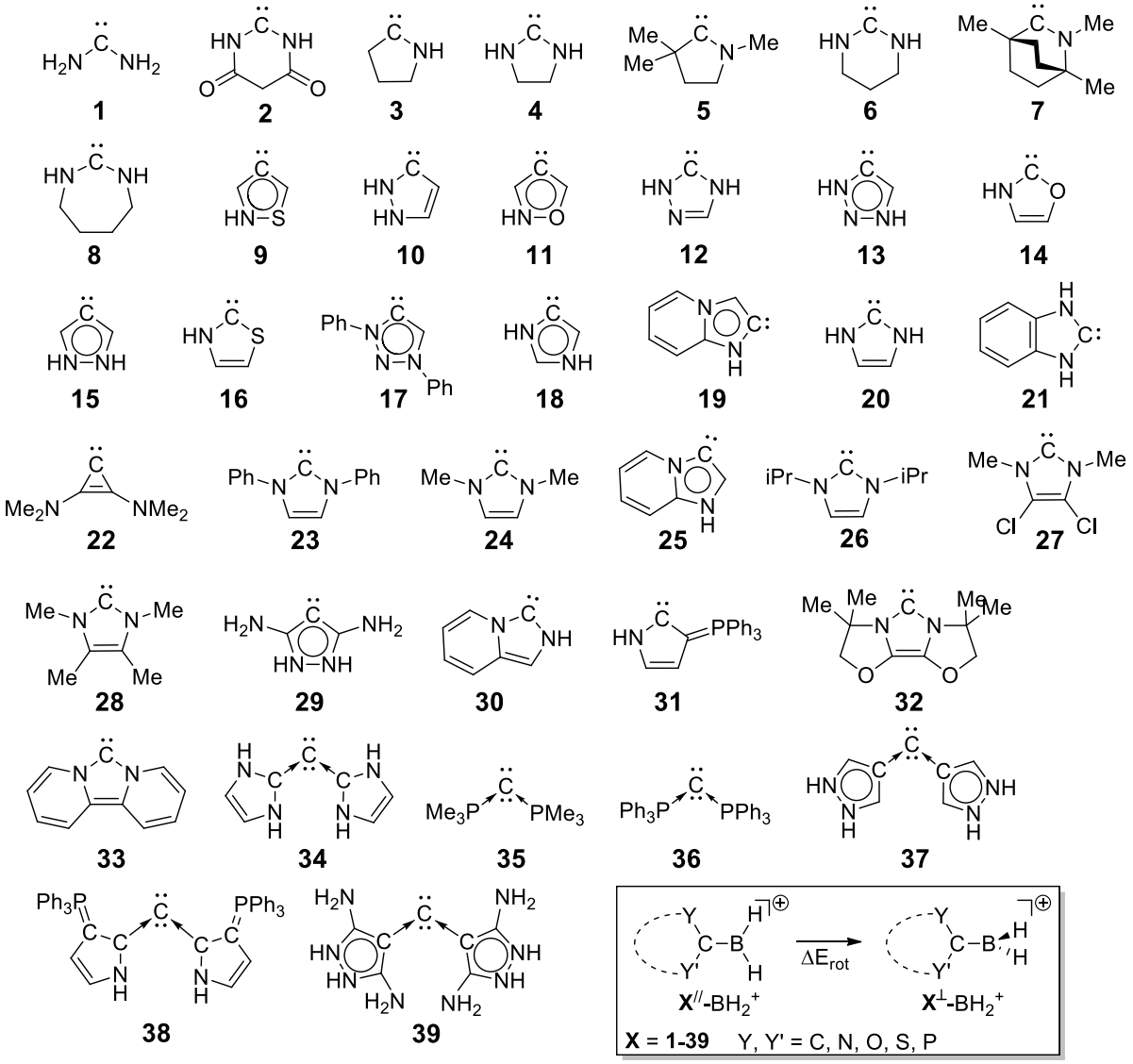

Scheme 2. **X**-BH_2^+ (X = **1**-**39**) borenium cation studied in this work.

π-bonding descriptors based on chemical insight

From the chemist's point of view, a double bond differs from a single bond by several features, in particular a shorter bond length and a significant energy barrier associated with the rotation around the bond. To estimate these characteristics, we calculated the energy barrier ΔE_{rot} associated with the rotation around the C-B bond, i.e. the energy required to go from $\mathbf{X}^{//}$-BH_2^+ to $\mathbf{X}^{\perp}$-BH_2^+ (Scheme 2). In all cases except **3**, **5** and **7**, $\mathbf{X}^{\perp}$-BH_2^+ is a transition state for this rotation and ΔE_{rot} has a positive value which range from 5 kJ/mol for **2** to 172 kJ/mol for **39**. For **3**, **5** and **7**, a negative value is obtained (between -29 and -13 kJ/mol) (see Table S1). This wide range of values confirms the structural diversity of compounds **1**-**39** in terms of π-donation capability. At the same time, the change from $\mathbf{X}^{//}$-BH_2^+ to $\mathbf{X}^{\perp}$-BH_2^+ induces in most cases, except for **1**-**5** and **7**, a slight increase in the B-C bond length, in line with the cancellation of the π-transfer to the vacant p_{vac}^{B} orbital, which is responsible for the partial double bond character.

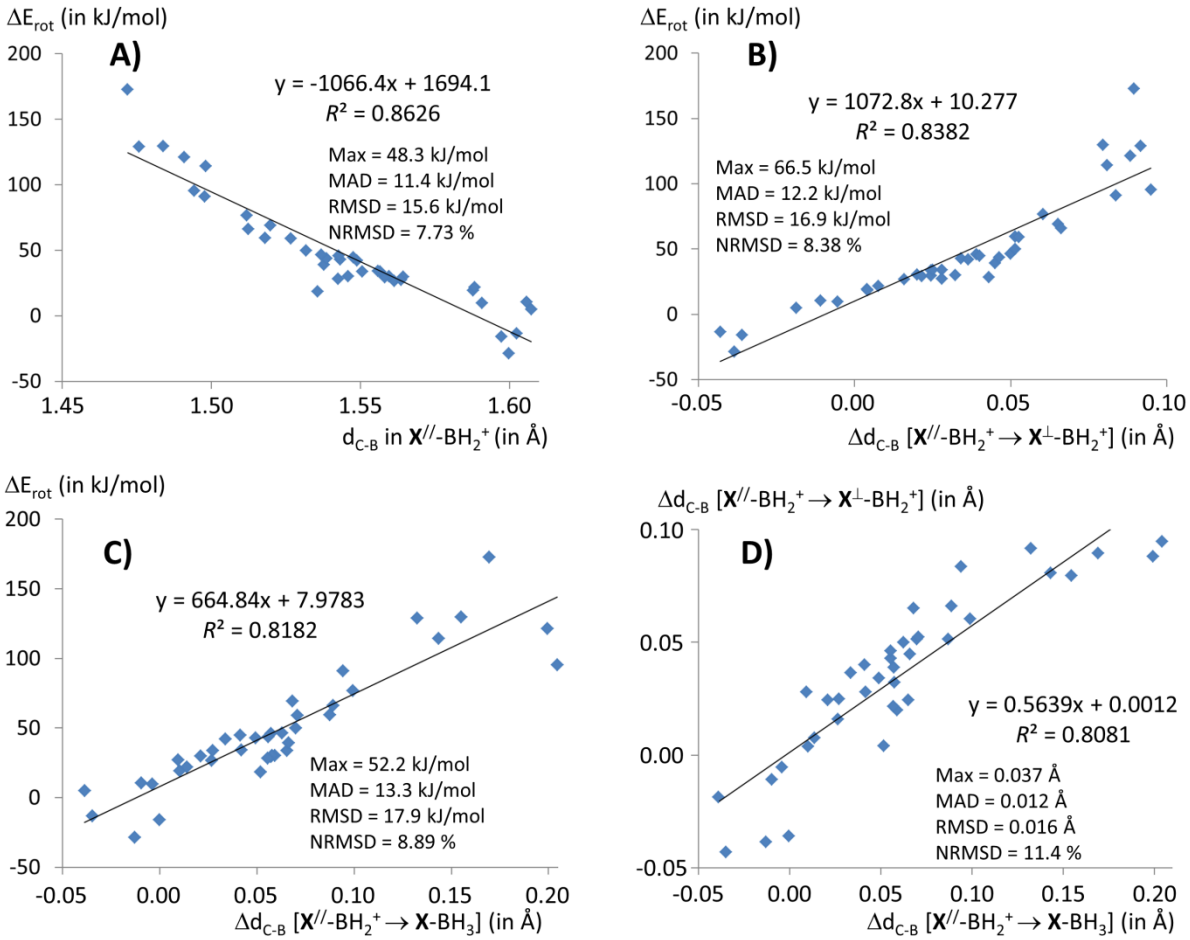

Figure 1. Correlation plots for **X**-BH_2^+ complexes computed at the B3LYP/TZVP level between: the energy barrier ΔE_{rot} associated with the rotation around the C-B bond *vs*. the C-B bond length ($d_{C\text{-}B}$) in $\mathbf{X}^{//}$-BH_2^+ (A); ΔE_{rot} *vs*. the change in the C-B bond length ($\Delta d_{C\text{-}B}$) when going from $\mathbf{X}^{//}$-BH_2^+ to $\mathbf{X}^{\perp}$-BH_2^+ (B) and **X**-BH_3 (C); $\Delta d_{C\text{-}B}$ when going from $\mathbf{X}^{//}$-BH_2^+ to $\mathbf{X}^{\perp}$-BH_2^+ *vs.* to **X**-BH_3 (D). Linear regression equation, coefficients of determination (R^2), maximum absolute deviations (Max), mean absolute deviations (MAD), root mean square deviations (RMSD) and normalized RMSD (NRMSD) are reported.

In agreement with the chemical expectation, Figure 1A indicates that there is a rough match between the C-B bond length ($d_{C\text{-}B}$) in $\mathbf{X}^{//}$-BH_2^+ and the energy barrier ΔE_{rot} associated with the rotation around the C-B bond. This correlation is only fairly good (R^2 = 0.86), indicating that these descriptors do not measure exactly the same chemical property. This discrepancy may be due to the fact that $d_{C\text{-}B}$ includes both the σ- and the π-interactions whereas ΔE_{rot} characterizes only the latter and measure an evolution from $\mathbf{X}^{//}$-BH_2^+ to $\mathbf{X}^{\perp}$-BH_2^+. In order to mitigate these differences, the C-B bond elongation $\Delta d_{C\text{-}B}$ during the rotation of the BH_2 group has been considered (Figure 1B). A correlation is again obtained, but it is not better than the one observed previously (R^2 = 0.84). A similar correlation (R^2 = 0.82, Figure 1C) is obtained by considering the C-B bond elongation when the H^- anion is added to $\mathbf{X}^{//}$-BH_2^+ to form the donor-acceptor **X**-BH_3 complex. The larger C-B bond length in **X**-BH_3 compared to $\mathbf{X}^{\perp}$-BH_2^+, as well as the moderately good correlation between $\Delta d_{C\text{-}B}$ to reach these two complexes from $\mathbf{X}^{//}$-BH_2^+ (R^2 = 0.81, Figure 1D), indicate that these two ways of considering a purely σ-bond are not equivalent. It is likely that the interaction between **X** and the rotated BH_2^+ or BH_3 groups in these complexes is not only a σ-interaction, but also includes other

component such as an electronic transfer from the **X** σ-system to the vacant p-orbital of the rotated BH_2^+ group in $\mathbf{X}^{\perp}$-BH_2^+ (*vide infra*).

π-bonding descriptors based on the NBO approach

In the framework of the NBO analysis, the C→B π-donation in $\mathbf{X}^{//}$-BH_2^+ complexes can be characterized through several indicators. First, we compute the WBI which is known to have good agreement with empirical bond order. Values of WBI between 0.83 ($\mathbf{2}^{//}$-BH_2^+) and 1.43 ($\mathbf{39}^{//}$-BH_2^+) have been obtained (Table S2). Comparisons between WBI and the C-B bond length show similar trend, but with moderate correlation (R^2 = 0.82. Figure S1). A better correlation is observed between WBI($\mathbf{X}^{//}$-BH_2^+) and ΔE_{rot} (R^2 = 0.90, Figure 2A). For $\mathbf{X}^{\perp}$-BH_2^+ complexes for which approximately a single C-B bond is expected, the WBI ranges as anticipated from 0.84 to 0.92. A revised π-bond order can be estimated by calculating the difference between the WBI obtained for $\mathbf{X}^{//}$-BH_2^+ and $\mathbf{X}^{\perp}$-BH_2^+ (ΔWBI).[101] ΔWBI lies between -0.06 and 0.50, which confirms the diverse π-donation capability of **1**-**39**. Small negative values are obtained for **3**, **5** and **7** for which the "perpendicular" conformer is more stable than the planar one. The ΔWBI parameter, which accounts for both the interaction in $\mathbf{X}^{//}$-BH_2^+ and $\mathbf{X}^{\perp}$-BH_2^+ complexes, as is the case with ΔE_{rot}, leads as expected to an improved but still imperfect correlation (R^2 = 0.92, Figure 2B).

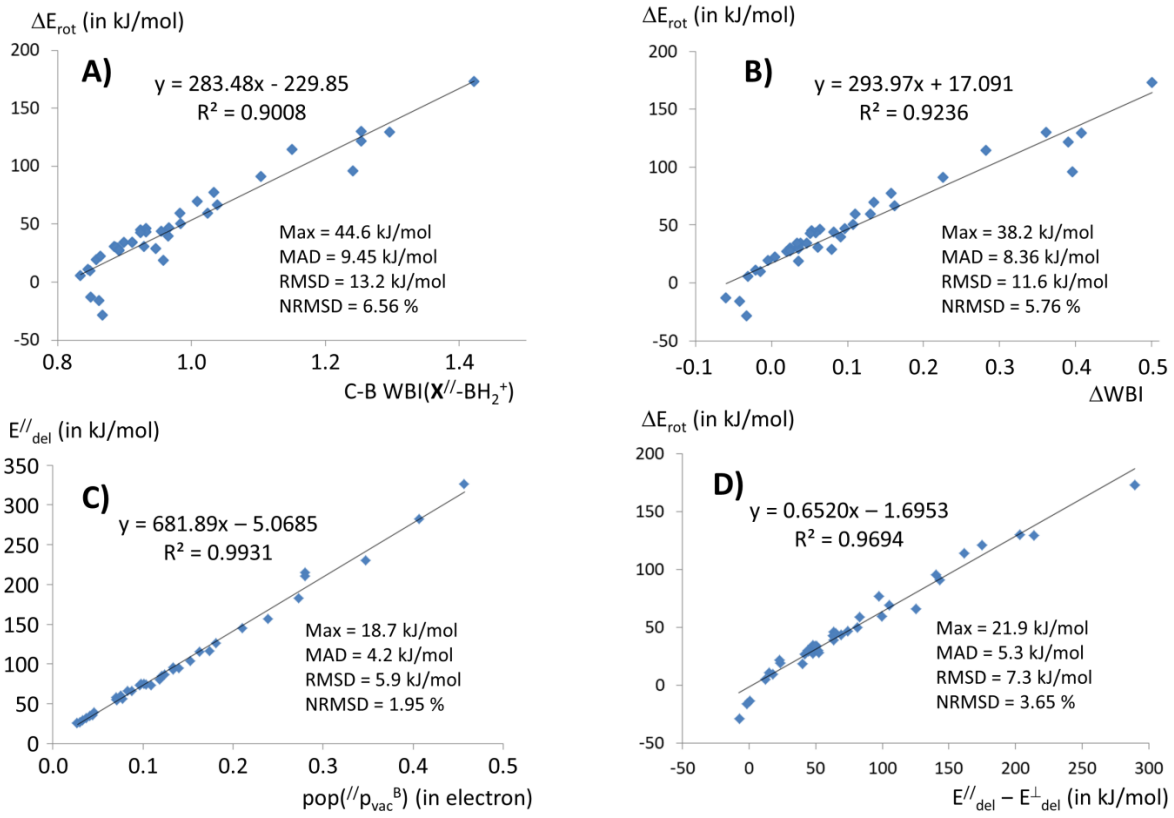

Figure 2. Correlation plots for **X**-BH_2^+ complexes computed at the B3LYP/TZVP level between various descriptors obtained with the NBO method.

WBI has been originally built as a quantitative measure of the electronic population occupying bonding molecular orbital.[9] Similarly, the electronic population of the p_{vac}^B orbital, noted as pop($^{//}p_{vac}^B$), is expected to measure the π-donation strength from **X** to BH_2^+ in $\mathbf{X}^{//}$-BH_2^+ complexes. Indeed, by construction, the p_{vac}^B orbital is utterly empty for the BH_2^+ fragment alone, whereas in the $\mathbf{X}^{//}$-BH_2^+ conformation, its population can only come from the π-type orbitals of the **X** moiety.

Pop($^{//}p_{vac}^{B}$) values range from 0.027 to 0.457 electron (see Table S2), again illustrating the diversity of π-donation properties of ligands **1**-**39**. The NBO6 program includes a module that allows to remove specific electronic interactions and to measure their energy contribution (see Computational Methods for details). This "deletion" energy, noted $E^{//}_{del}$, has also been computed for the $\mathbf{X}^{//}$-BH_2^+ conformer by removing the p_{vac}^{B} orbital, thus cancelling any possibility of π-electronic donation from **X** to BH_2^+. It is noteworthy that pop($^{//}p_{vac}^{B}$) and $E^{//}_{del}$ correlate almost perfectly with each other (R^2 = 0.99, Figure 2C). These NBO electronic population and energetic parameters therefore measure the same chemical property that will herafter be referred to as the *intrinsic* strength of the π-interaction. This outstanding linear correlation is nevertheless expected to be restrained to bonds between two defined atoms, here boron and carbon atoms, and probably cannot be extended to all bonds (see Computational Methods). To a lesser extent, the WBI allows also a suitable quantification of the *intrinsic* π-bond, as very good correlation between the C-B bond WBI and either pop($^{//}p_{vac}^{B}$) or $E^{//}_{del}$ is observed ($R^2 > 0.975$, Figure S2).

The above parameters calculated with the NBO method do not correlate satisfactorily with the previously calculated descriptors based on chemical insight. Indeed, an R^2 value of 0.91 is obtained when comparing ΔE_{rot} and pop($^{//}p_{vac}^{B}$) or $E^{//}_{del}$ (Figure S2). This reveals the conceptual difference between the *intrinsic* and the *relative* strength of the π-interaction. The latter, measured by ΔE_{rot}, results from the energy difference between the planar ($\mathbf{X}^{//}$-BH_2^+) and the perpendicular ($\mathbf{X}^{\perp}$-BH_2^+) conformations. To confirm this assumption, the $\mathbf{X}^{\perp}$-BH_2^+ conformers have been used to compute the pop($^{\perp}p_{vac}^{B}$) and $E^{\perp}_{del}$ values (Table S3). In the $\mathbf{X}^{\perp}$-BH_2^+ conformation, the p_{vac}^{B} orbital is coplanar with the **X** moiety and perpendicular to the B-C bond, inducing non-zero overlap between this p orbital and the σ backbone of **X**. The pop($^{\perp}p_{vac}^{B}$) values, which range between 0.006 and 0.071 electron, reveals weak in-plane π-type electronic donation from **X** to p_{vac}^{B}, in agreement with our previous assessment. The deletion of this p orbital leads to $E^{\perp}_{del}$ which nicely correlate with pop($^{\perp}p_{vac}^{B}$) (R^2 = 0.94, Figure S3). Assuming that the interactions between the B-H bonds and the σ-system of **X** in $\mathbf{X}^{//}$-BH_2^+ and those between the B-H bonds and the π-system of **X** in $\mathbf{X}^{\perp}$-BH_2^+ are weak (or similar), and that the B-C σ-bond strength is weakly affected by the rotation of the BH_2 group, ΔE_{rot} is expected to be equivalent to the difference between $E^{//}_{del}$ and $E^{\perp}_{del}$. This is nicely confirmed by the very good correlation obtained between ΔE_{rot} and ($E^{//}_{del} - E^{\perp}_{del}$) ($R^2$ = 0.97, Figure 2D). The descriptors $\Delta E_{del} = E^{//}_{del} - E^{\perp}_{del}$ and $\Delta pop(p_{vac}^{B}) = pop(^{//}p_{vac}^{B}) - pop(^{\perp}p_{vac}^{B})$ are therefore reliable measures of the *relative* strength of the π-interaction, whose reference is ΔE_{rot} (see also Figure S3). It should be noted that the absolute values of ΔE_{rot} and ΔE_{del} are different, the former being significantly lower than the latter. Features of the NBO approach, which allows only bonding interactions to be calculated and does not cover antibonding contributions,[102] explains the systematic overestimation of ΔE_{del}.

π-bonding descriptors based on the ETS-NOCV approach

The ETS-NOCV method allows to calculate the energy and to identify the nature of the different orbital interactions between two fragments. Diagonalization of the deformation density matrix due to bonding provides eigenvectors named natural orbitals for chemical valence (NOCVs). Pairs of NOCV, having opposite eigenvalues υ_i and $-\upsilon_i$ and for which an energy ΔE_i is associated, are obtained. They enable to visualize the deformation of the density associated with each interaction and to determine its nature. Therefore, the total orbital interaction between fragments is partitioned into several chemically interpretable interactions ($NOCV_i$) for which energy (ΔE_i) and charge transfer (υ_i) are quantified.

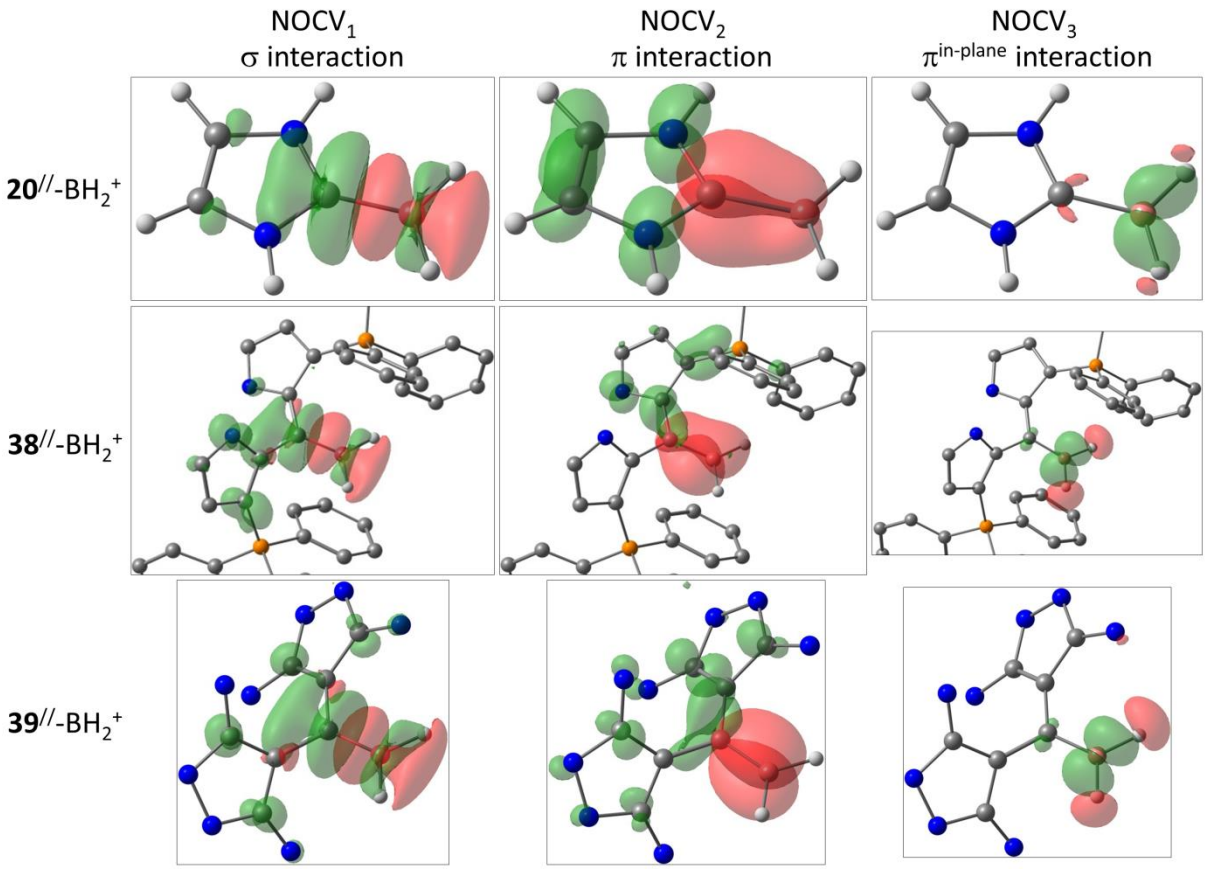

Figure 3. Deformation densities associated with the orbital interactions in $\mathbf{X}^{//}$-BH_2^+ (**X** = **20**, **38** and **39**). The charge flow of the electronic density is green → red. For **X**=**38** and **39**, H atoms, except BH_2, have been omitted for clarity. Isosurface value: 0.003 a.u.

All $\mathbf{X}^{//}$-BH_2^+ complexes showed similar features regarding the description of the bonding between C-donor and borenium within $\mathbf{X}^{//}$-BH_2^+. Three main contributions accounting for about 90% of the total orbital interaction (Table S4) can be identified in the deformation density (Figure 3). The first pair of NOCV, $NOCV_1$, is the strongest contribution. It corresponds to a σ-type interaction which can be described as the $\mathbf{X}\rightarrow BH_2^+$ σ-donation. The second deformation density $NOCV_2$ displays a π-type interaction: the π charge flow from the C-donor ligand to the vacant p orbital of the boron atom suggests that it corresponds to the π-donation. The third contribution $NOCV_3$ corresponds to a π-type interaction located in the Y_2C-BH_2 plane.

Surprisingly, neither the flow of electron density associated with the π-donation, $\Delta q^{//}_{\pi} = \upsilon^{//}_2$, nor the energy associated with the π-donation interaction, $\Delta E^{//}_{\pi} = \Delta E^{//}_2$, provide a very good correlation with $pop(^{//}p_{vac}{}^{B})$ or $E^{//}_{del}$, respectively (Figures 4A and S4). Do these non-perfect correlations illustrate a disagreement between the NBO and ETS-NOCV methods? It should be noted that the π-type interaction corresponding to the second deformation density has been shown to include not only the contribution of the π-donation but also the π-polarization of the C-donor fragment, i.e. the reorganization of π-electron density inside **X** due to the formation of the σ-bond.[95] Thus, the previous non-satisfactory correlations could also be explained by a misinterpretation of the ETS-NOCV results. To investigate this hypothesis, the ETS-NOCV π-donation energy ($\Delta E^{//}_{\pi}$) calculated for $\mathbf{X}^{//}$-BH_2^+ complexes by deduction from $\Delta E^{//}_{\pi}$ has been adjusted. The corrected ETS-NOCV π-donation energy ($\Delta E^{//}_{\pi\,corr}$) is obtained by deduction of the π-contribution calculated by the same approach for **X**-H^+ complexes from $\Delta E^{//}_{\pi}$ (Table S5 and Figure S5).[95] Satisfyingly, a much better linear correlation is

obtained between $\Delta E^{//}{}_{\pi\ corr}$ and $E^{//}{}_{del}$. The only outlier is the **38**$^{//}$-BH_2^+ complex and by excluding this complex the correlation is excellent (R^2 = 0.99, Figure 4B), which validates the hypothesis and demonstrates that the intrinsic strength of the π-interaction can also be calculated by the ETS-NOCV method provided that the polarization of the fragments is taken into account. Similarly, a strong quadratic correlation is obtained between pop($^{//}p_{vac}^{B}$) and $\Delta q^{//}{}_{\pi\ corr} = \upsilon^{//}{}_2 - \upsilon_2$(**X**-H$^+$) ($R^2$ = 0.99, Figure S4).

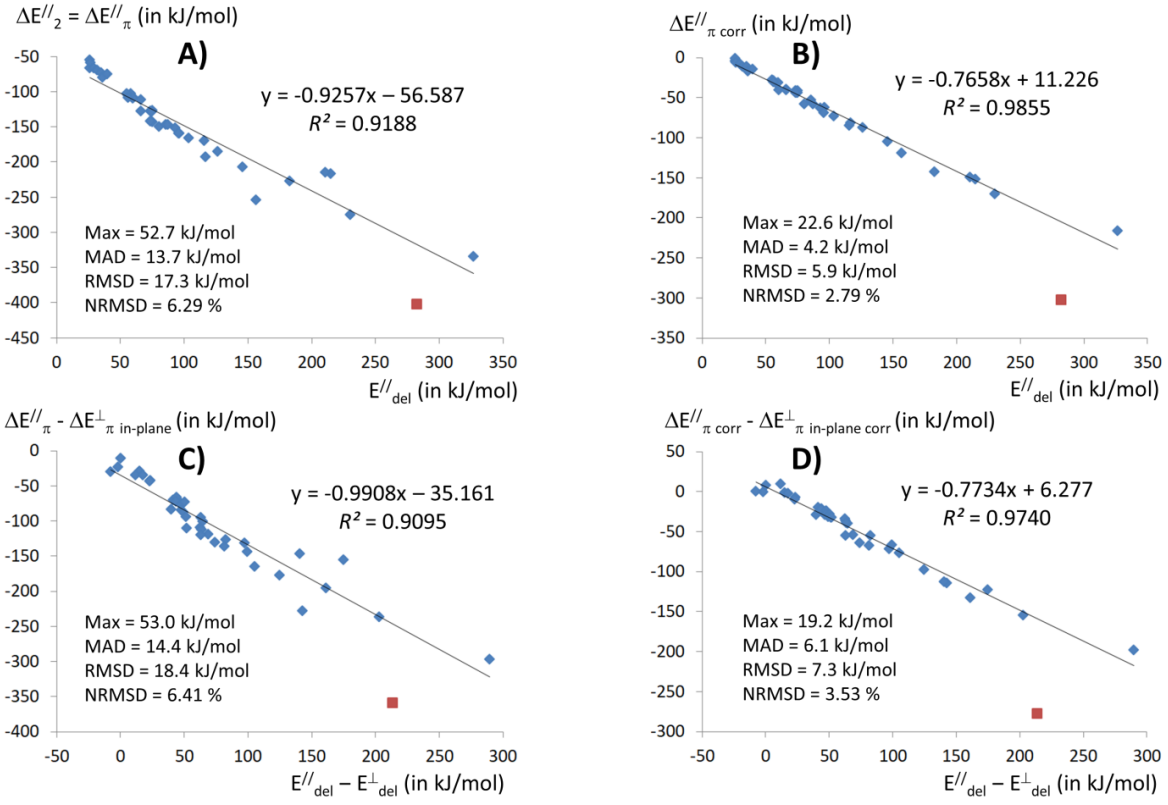

Figure 4. Correlation plots for **X**-BH_2^+ complexes between various descriptors obtained with the NBO and ETS-NOCV methods, where the brown square corresponds to **X** = **38** and is not included in the trendlines.

Analysis of deformation densities enables to explain the discrepancy observed for complex **38**$^{//}$-BH_2^+ with the ETS-NOCV method. With respect to the bisector plane of the **X**$^{//}$-BH_2^+ complexes, which is perpendicular to the complex plane and goes through the B-C axis, the deformation densities corresponding to the σ- and π-interactions (Figure 3) are symmetrical, in the sense that they involve both moieties of the C-donor ligand in an equivalent manner. This characteristic is observed for all complexes, except **38**$^{//}$-BH_2^+ for which the charge depletion of one moiety of **38** is observed only for $NOCV_1$, whereas the other part is involved only in $NOCV_2$ (Figure 3). Moreover, with respect to the plane defined by the C-BH_2 moiety, the inflow part of the deformation density in $NOCV_2$ for **38**$^{//}$-BH_2^+ is not perfectly symmetrical, contrary to what is observed for all other complexes. These visualizations suggest that $NOCV_1$ and $NOCV_2$ do not fit exactly with purely σ- and π-interactions, respectively, but that σ- and π-interactions are partly combined in these two NOCVs. Thus, the σ-interaction in **38**$^{//}$-BH_2^+ would be underestimated, while the π-interaction would be overestimated, explaining its outlier behavior.

The same polarization correction approach can be used to estimate the *relative* strength of the π-interaction through the ETS-NOCV method. To that end, the ETS-NOCV $\pi^{in\text{-}plane}$-donation energy

($\Delta E^{\perp}_{\pi\ in\text{-}plane}$) has been calculated for $\mathbf{X}^{\perp}$-BH_2^+ complexes (Table S6 and Figure S5). Without correction of the polarization, $E^{//}_{del} - E^{\perp}_{del}$ and ΔE_{rot} correlates modestly with $\Delta E^{//}_{\pi} - \Delta E^{\perp}_{\pi\ in\text{-}plane}$ (R^2 = 0.91, Figures 4C and S4). The correlation is improved significantly by applying a polarization correcting on $\Delta E^{//}_{\pi}$ and $\Delta E^{\perp}_{\pi\ in\text{-}plane}$ (R^2 = 0.97, Figures 4D and S4).

π-bonding descriptors based on the QTAIM approach

The QTAIM method provides the possibility of estimating the π-bond strength using different descriptors, which can be either local or global. Local chemical indexes include the charge density ρ and the ellipticity ε derived from characteristics of the density at the bond critical point (bcp), and the Delocalization Index (DI) corresponds to the global index. It is well known that ρ_{bcp} and DI can be used to estimate the bond order.[103-105] More precisely, a logarithmic relationship was proposed between ρ_{bcp} and the bond order estimated by DI:[104] $DI = \exp[A(\rho_{bcp} - B)]$. At the B3LYP/TZVP level of calculation, the data points for the C-B bond in the 39 $\mathbf{X}^{//}$-BH_2^+ complexes fit reasonably well to this equation with A = 10.4644, B = 0.1725 and R^2 = 0.92. A quadratic regression slightly improves the correlation with R^2 = 0.94 (Figure S6). Comparison between indexes $\rho^{//}_{bcp}$ or $DI^{//}$ and those previously calculated clearly shows that the delocalization index provides more valuable information. This is reflected in a good linear correlation between $DI^{//}$ and $E^{//}_{del}$ (R^2 = 0.94, Figure 5A). Other measures of the *intrinsic* strength of the π-interaction, such as $pop(^{//}p_{vac}{}^{B})$ and $\Delta E^{//}_{\pi\ corr}$ give similar correlation with respect to $DI^{//}$ (respectively R^2 = 0.95 and 0.94 excluding **38**$^{//}$-BH_2^+, Figure S6). Conversely, other indicators, such as $d_{C\text{-}B}$, $\Delta E^{//}_{\pi}$ or ΔE_{rot} for which a lower performance for estimating the *intrinsic* strength of the π-interaction has been shown above, give lower correlations (R^2 = 0.88, 0.92 and 0.92, respectively, not displayed). Similarly, ΔDI, calculated as the difference between the delocalization indexes $DI^{//}$ and $DI^{\perp}$ computed respectively for $\mathbf{X}^{//}$-BH_2^+ and $\mathbf{X}^{\perp}$-BH_2^+, turns out to be a good measure of the *relative* strength of the π-interaction, as revealed by the good correlation between ΔDI and ΔE_{rot} (R^2 = 0.96, Figure 5B).

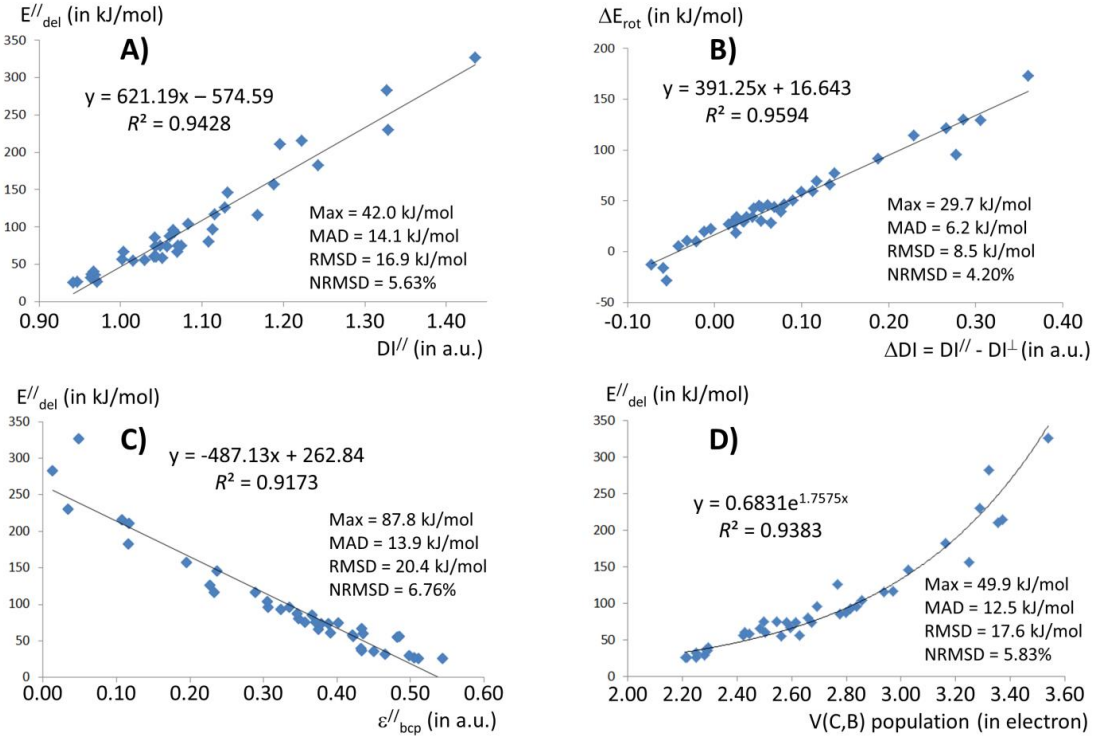

Figure 5. Correlation plots for **X**-BH_2^+ complexes between various descriptors obtained with the DFT, QTAIM, ELF and NBO methods.

The ellipticity of the electron density at the bond critical points, ε_{bcp}, is a parameter computed in the framework of the AIM analysis.[106] This parameter provides a quantitative measurement of the anisotropy of the electron density at the bcp. This measure of the deviation of the charge distribution of the bond from axial symmetry is provided by the ratio between the two negative curvatures λ_1 and λ_2 of ρ at the bond critical point: $\varepsilon_{bcp} = \lambda_1 / \lambda_2 - 1$ (with $|\lambda_1| > |\lambda_2|$). Therefore, the ellipticity has been logically associated with the π character of bonds. For a single bond, $\varepsilon_{bcp} = 0$ because $\lambda_1 = \lambda_2$. For double bonds, the decrease of the density in the direction of the π-system should be smaller than that in the σ-plane of the bond. Consequently, the π-direction defines the λ_2 curvature which leads to $\varepsilon_{bcp} > 0$, ε_{bcp} being at maximum for bonds of order 2. On this basis, it seems satisfactory to obtain a significant linear correlation between ε_{bcp} and $E^{//}_{del}$ (R^2 = 0.92, Figure 5C). This trend is however highly surprising because an ellipticity close to zero is obtained for molecules which possess a large π-interaction whereas molecules with low $E^{//}_{del}$ values show large ε_{bcp} values.

In order to explain this unexpected result, we focus our study on **1**$^{//}$-BH_2^+, **21**$^{//}$-BH_2^+ and **37**$^{//}$-BH_2^+, which respectively show small, medium and large π-interaction. The calculation for these complexes of the ellipticity $\varepsilon(d) = \lambda_1(d) / \lambda_2(d) - 1$ (with $|\lambda_1(d)| > |\lambda_2(d)|$) along the C-B bond, at the distance d from the C atom, reveals two maxima around d = 0.4 and 1.1 Å separated by a minimum value close to zero and located near the middle of the C-B bond (Figure 6). A similar result is obtained for the planar conformation of CH_2-BH_2^+ which possesses a pure σ-CB bond as its π-system is empty. On the other hand, this result differs strongly from what is obtained for the CC double bond in CH_2=CH_2 or the CB double bond in CH_2=BH_2^-, for which a single maximum is calculated along the bond.

These findings are explained by a thorough examination of the negative eigenvalues $\lambda_1(d)$ and $\lambda_2(d)$ ($|\lambda_1(d)| > |\lambda_2(d)|$) of $\Delta\rho(d)$ along the bond. For the sake of clarity, the curvature of $\rho(d)$ along the π direction is named $\lambda_\pi(d)$, while the curvature in the plane of the molecule along the axis perpendicular to the bond is noted $\lambda_{\pi\ in\text{-}plane}(d)$. We also define $\varepsilon_{corr}(d) = \lambda_{\pi\ in\text{-}plane}(d) / \lambda_\pi(d) - 1$. For CH_2=CH_2 and CH_2=BH_2^-, as expected, $\lambda_2(d) = \lambda_\pi(d)$ at the bcp and its neighbourhood, which means that $\varepsilon(d) = \varepsilon_{corr}(d)$ (Figure 6). However, this is not the case close to the bond ends where $\lambda_1(d) = \lambda_\pi(d)$ and $\varepsilon(d) \neq \varepsilon_{corr}(d)$. More precisely, $\varepsilon_{corr}(d)$ turns negative, which is an indication that the decrease of the density is faster in the π-direction than in the plane of the molecule. We assume that this is due to the proximity of the C-H and B-H σ-bond. This assumption enables us to explain the 2 maxima of $\varepsilon(d)$ obtained for CH_2-BH_2^+, which do not reflect any π system of the molecule but the presence of the C-H and B-H bonds at both bond ends. As the C-B bond is polarized, due to the low boron electronegativity, the bcp is located approximately at 2/3 of the CB bond, on the boron side, i.e. in the region of greatest influence of the B-H bonds. ε_{bcp} is thus large even if the C-B bond in CH_2-BH_2^+ is not a double bond. The influence of the rising π-donation from **1**$^{//}$-BH_2^+ to **21**$^{//}$-BH_2^+ and **37**$^{//}$-BH_2^+ is thus clearly visible when calculating $\varepsilon_{corr}(d)$ along the B-C axis, with an increasing maximum located on the C atom side. The local character of ε_{bcp} does not allow this feature to be distinguished, and, on the contrary, this descriptor can be misleading because it does not distinguish the direction of the curvatures λ_1 and λ_2. Attempts to use $\varepsilon_{corr}(d)$ as a π-bond descriptor were unsuccessful. With respect to $E^{//}_{del}$, the best correlation, using the maximum of $\varepsilon_{corr}(d)$, gives only a poor correlation with R^2 = 0.79 (Figure S6).

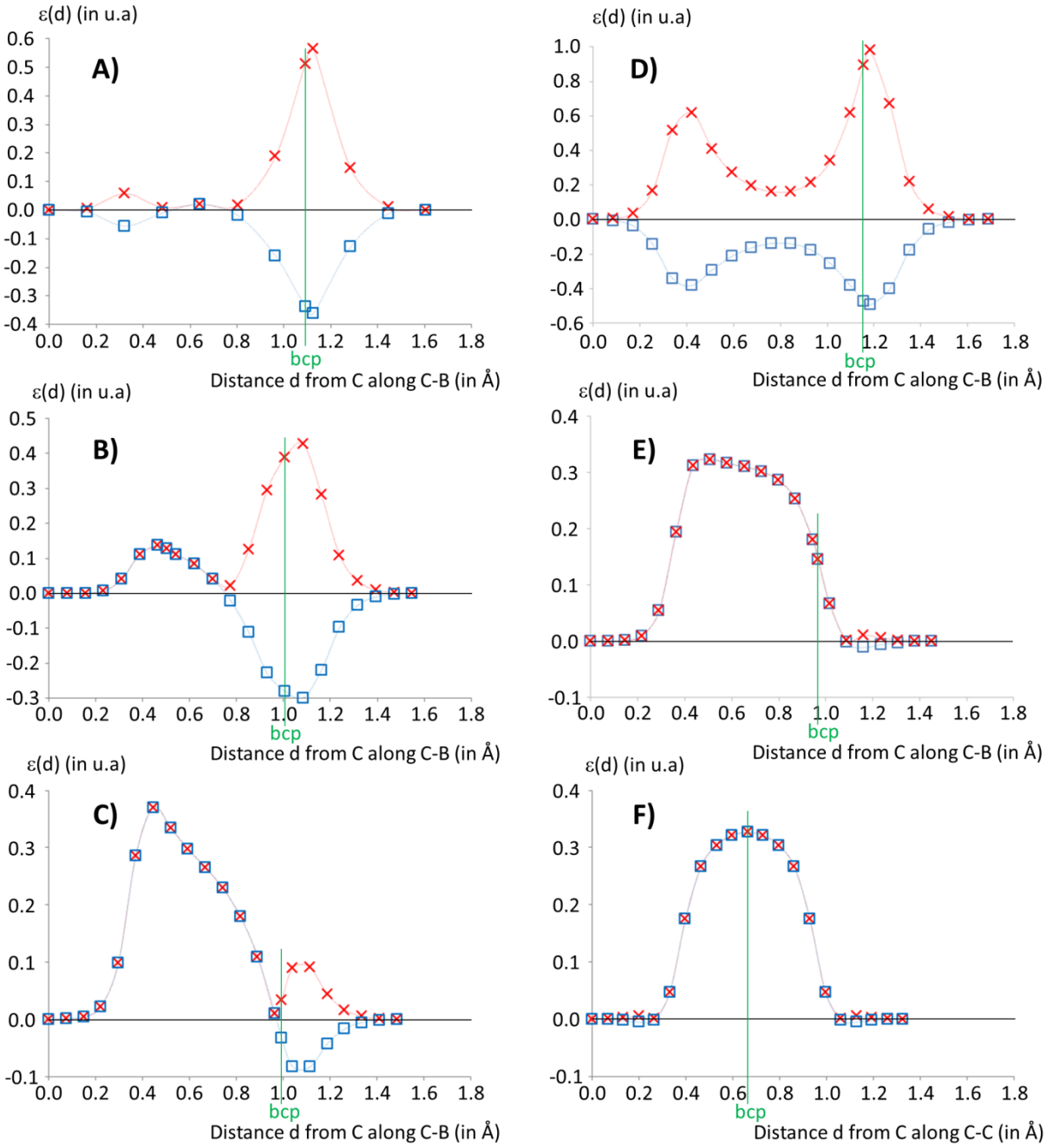

Figure 6. Variation of ellipticity indices $\varepsilon(d) = \lambda_1(d) / \lambda_2(d) - 1$ (with $|\lambda_1(d)| > |\lambda_2(d)|$) (red cross) and $\varepsilon_{corr}(d) = \lambda_{\pi\ in\text{-}plane}(d) / \lambda_{\pi}(d) - 1$ (blue square), calculated at the distance d from the C atom along the C-B or C-C bond for A) $\mathbf{1}^{//}$-BH_2^+, B) $\mathbf{21}^{//}$-BH_2^+, C) $\mathbf{37}^{//}$-BH_2^+, D) $CH_2^{//}$-BH_2^+, E) CH_2=BH_2^- and F) CH_2=CH_2.

π-bonding descriptors based on the ELF approach

The topological analysis of the electron localization function (ELF) provides a partition of the molecular space into core and valence basins. This method allows the study of chemical bonds as a one-to-one correspondence between the valence basins, and lone pairs or Lewis-type bonds has been achieved.[21] Integration of the electronic density over the basin corresponding to the C-B bond, V(C,B), is used to calculate the population of the C-B bond in $\mathbf{X}^{//}$-BH_2^+, $pop^{//}[V(C,B)]$. As expected, this population reflects the *intrinsic* π character of the bond, as shown by the correlation with $E^{//}_{del}$. The best fit is obtained with a logarithmic relationship (R^2 = 0.94, Figure 5D). Calculation of the difference in the population of the C-B bond in $\mathbf{X}^{//}$-BH_2^+ and $\mathbf{X}^{\perp}$-BH_2^+, $\Delta pop = pop^{//}[V(C,B)] - pop^{\perp}[V(C,B)]$, gives a

much weaker correlation with respect to ΔE_{rot} (R^2 = 0.81, Figure S6), showing that Δpop is not a good descriptor for measuring the *relative* strength of the π-interaction.

Conclusion

In the course of this work, the comparison between five modeling approaches (DFT, NBO, ETS-NOCV, QTAIM and ELF) for estimating the magnitude of the π-donation has been achieved. Chemical systems, combining various divalent C-donor ligands with a BH_2^+ borenium group, have been designed. They include a partial CB π-bond resulting from a π-donation that is not biased by any other π-interaction between the two fragments and toward the boron atom. The intensity of the π-bond has been estimated from a wide selection of indicators and compared with each other. The different modelling methods enable the calculation of π-bond descriptors which correlate very well with each other (R^2 between 0.94 and 0.99) and therefore appear to describe the same chemical property. However, such correlations require adjustments from the standard calculations commonly used in the literature, in particular for ETS-NOCV and QTAIM approaches. The use of these methods without these corrections leads to lower correlations (R^2 < 0.92), or even to disagreements that may suggest that these methods diverge, which is not the case. In detail, the conclusions are as follows:

- A π-bond is characterized by 2 families of indicators: *intrinsic* and *relative* π-bond strength descriptors. Correlations between these two families are moderate (R^2 around 0.90).
- *Intrinsic* indicators describe the intensity of the π-bond in the molecule under study, whereas *relative* indicators measure the difference between the molecule with the π-interaction and the same molecule in a conformation which prevents this interaction.
- The reference *relative* indicator is the rotational barrier around the π-bond ΔE_{rot}. The bond lengths give at best an approximate indication of the strength of the π-bond.
- The NBO method provides three descriptors with moderately good (Wiberg Bond Index WBI) to very good (atomic π-population and NBO energetic analysis through the deletion of selected NBOs) performance to measure the π-bond strength. However, the absolute value of the π-bond energy is systematically overestimated by this approach.
- The π-donation-type NOCV eigenvalue and energy failed to give reliable measure of the π-bond strength. A significantly enhanced accuracy is obtained by correcting the previous values from the polarization of the π-system associated with the π-interaction, showing that NOCV chemical interpretation should be made with caution.
- Although the ETS-NOCV approach does not usually require symmetrical molecules to dissociate σ- and π-contributions, a case has been identified where this method fails and mixes σ- and π-interactions.
- The Delocalization Index (DI) provided by the QTAIM approach reproduces accurately the π-bond strength, contrary to the density value at the bond critical point ρ_{bcp}, which gives less relevant correlations. The ellipticity ε_{bcp} fails drastically for these dative π-bonds, due to the influence of the neighboring σ-bonds which reverse the role of the eigenvalues of the density curvature.
- The bond population given by the ELF method gives a reasonable correlation, but only for the *intrinsic* π-bond strength.

All these correlations have been obtained for a single type of π-interaction between C and B atoms. Further work will be carried out in the future to investigate whether or not these correlations could be extended to other bonds, in particular for the NBO method.

Computational methods

Calculations were carried out with the Gaussian09 package[107] and all structures were fully optimized without any symmetry constraints at the DFT level by means of the B3LYP functional.[108,109] The TZVP basis set[110,111] was applied for all atoms. Each stationary point has been characterized with frequency analysis and shows the correct number of negative eigenvalues (zero for a local minimum and one for a transition state). To get accurate geometries and energies, the SCF convergence criterion was systematically tightened to 10^{-8} au, and the force minimizations were carried out until the rms force became smaller that (at least) 1 x 10^{-5} au ("tight" optimization keyword in Gaussian 09). The "UltraFine" grid (99 radial shells and 590 angular points per shell) was used throughout the calculations, as recommended when using Gaussian 09. This level of calculation has been shown to give very accurate binding energies for both NHC-BH_2^+ and NHC-H^+ complexes.[95] Furthermore, in order to ensure that the results obtained are not dependent on the level of calculation used, geometry optimizations were also carried out for all $\mathbf{X}^{//}$-BH_2^+ and $\mathbf{X}^{\perp}$-BH_2^+ complexes with the M06 functional[112] and the 6-311G(d,p)[113,114] basis set. The results obtained, concerning bond lengths, ΔE_{rot} energy barrier or NBO analysis, show an excellent agreement between B3LYP and M06 data (see Tables S1-S3), therefore only B3LYP data are presented in the text.

Electronic structures obtained at the B3LYP/TZVP level were explored by means of natural bond orbital (NBO) analysis[18] using the NBO6 program.[115,116] The NBO method is a multistep localization process which provides a quantitative description of the electronic structure in terms of natural atomic orbitals (NAOs) and natural bond orbitals (NBOs). NBOs are localized 1- or 2-center orbitals which give the 'best' Lewis structure corresponding to the total electron density. In all $\mathbf{X}^{//}$-BH_2^+ and $\mathbf{X}^{\perp}$-BH_2^+ complexes, the boron atom is involved in 7 or 8 valence Lewis and non-Lewis NBOs. This includes 2 σ_{BH} bonding and 2 σ^*_{BH} antibonding orbitals, 1 σ_{CB} bonding and 1 σ^*_{CB} antibonding orbitals, and either 1 unfilled valence nonbonding orbital of 'lone vacancy' type (LV(B)) or 1 π_{CB} bonding and 1 π^*_{CB} antibonding orbitals. The occupancy-weighted symmetric orthogonalization method used to generate the NAOs allows to compute the Wiberg bond index (WBI).[9] In planar $\mathbf{X}^{//}$-BH_2^+ complexes located in the xOy plane, the occupancy of the p_z NAOs of the boron atom provides the electronic population of the vacant p orbital of this atom, noted pop($^{//}p_{vac}^{B}$).[96,117] Alternatively, the occupancy and polarization of the appropriate π_{CB}/π^*_{CB} or LV(B) NBOs allows to compute the electronic population of the vacant p orbital of B in $\mathbf{X}^{//}$-BH_2^+ (pop($^{//}p_{vac}^{B}$)) and $\mathbf{X}^{\perp}$-BH_2^+ (pop($^{\perp}p_{vac}^{B}$)) complexes. These two approaches to compute pop($^{//}p_{vac}^{B}$) give similar values.

The strength of donor–acceptor interaction between selected fragments can be quantified by examining possible interactions between occupied (donor) Lewis NBOs and unoccupied (acceptor) non-Lewis NBOs. Second-order perturbation theory in the NBO basis allows evaluating their energetic importance. Using this well-known approach to estimate the π-donation of **X** to the vacant p-orbital of BH_2^+ requires the NBO method to provide a Lewis structure with a LV(B) NBOs on the boron atom. For $\mathbf{X}^{//}$-BH_2^+ complexes for which this is not the case, the $choose keyword has been used to specify a Lewis structure that is as close as possible to the 'best' Lewis structure and that satisfies this condition. The π-system of **X** determines the donor Lewis NBOs. Depending on the nature of **X**, these NBOs are diverse, including lone pair on the C atom or C=C or C=N π-bond. Due to the π-delocalization for many **X** moieties, several set of NBOs that describe roughly the same percentage of the total electron density can adequately describe their π-system. However, various tests carried out with different set of NBOs show that the donor-acceptor interaction energy between the π-system of **X** and LV(B) provided by the second-order perturbation theory strongly depends on the set of NBOs used to describe the π-system of **X** (see Table S8). The second-order

perturbation theory approach therefore leads to results that do not allow a consistent comparison of all $\mathbf{X}^{//}$-BH_2^+ complexes. An alternative is provided by the \$del option of NBO6, which allows to determine the energetic effect of deleting certain NBOs. This approach has been used to calculate $E^{//}_{del}$ for $\mathbf{X}^{//}$-BH_2^+ and $E^{\perp}_{del}$ for $\mathbf{X}^{\perp}$-BH_2^+. In all cases, the LV(B) NBO has been deleted, as well as the Rydberg orbitals located on B having the same spatial direction as LV(B) and subject to a significant increase in their electronic population when only the LV(B) NBO is deleted.

The NBO donor-acceptor perturbation theory gives an explanation for the linear dependency between an energetic parameter ($E^{//}_{del}$) and an electronic population parameter ($pop(^{//}p_{vac}^{B})$). A linear correlation has been previously noticed between "deletion" energy and second-order stabilization energy E(2) between an occupied NBO ϕ^0_i of energy ε^0_i and an unoccupied NBO ϕ^0_j of energy ε^0_j : $E(2) = -pop(\phi^0_i) * < \phi^0_i \ |F| \ \phi^0_j >^2 / (\varepsilon^0_j-\varepsilon^0_i)$, in which F is the 1-electron Kohn-Sham Hamiltonien.[18] The overlap between ϕ^0_i and ϕ^0_j leads to a bonding (ϕ^+) and an antibonding (ϕ^-) orbitals, with $\phi^+ = c_i \phi^0_i + c_j \phi^0_j$. Perturbation theory indicates that $\phi^+ = A^* [\phi^0_i + \phi^0_j * < \phi^0_i \ |F| \ \phi^0_j > / (\varepsilon^0_j-\varepsilon^0_i)]$. The electronic transfer from ϕ^0_i to ϕ^0_j associated to this perturbation is given by $c_j^2 = A^2 * < \phi^0_i \ |F| \ \phi^0_j >^2 / (\varepsilon^0_j-\varepsilon^0_i)^2 = c_i^2 * E(2) / [pop(\phi^0_i) * (\varepsilon^0_j-\varepsilon^0_i)]$. For a weak perturbation, $c_i^2 \approx pop(\phi^0_i)$. Considering that ϕ^0_i and ϕ^0_j are located on the C and B atoms respectively, $(\varepsilon^0_j-\varepsilon^0_i)$ remains approximately constant. Therefore, in case of the π-donation of a C-donor ligand **X** into the BH_2^+ borenium, c_j^2 corresponds to the π-population at the B atom $pop(^{//}p_{vac}^{B})$ and is linearly dependent with respect to E(2), and thus to $E^{//}_{del}$.

An energy decomposition analysis (EDA)[28] of the C-B and C-H bonds in $\mathbf{X}^{//}$-BH_2^+, $\mathbf{X}^{\perp}$-BH_2^+ and **X**-H^+ complexes was done at the B3LYP level by using the extended transition state (ETS) scheme[26,27] with the ADF2017 program[118-120] based on the B3LYP/TZVP geometries. All elements were described by basis sets of triple-ξ quality augmented by two sets of polarisation functions (basis set called TZ2P in ADF).[121] Core electrons (1s for boron, carbon, nitrogen and oxygen atoms, [He]2s2p for phosphorus, sulfur and chlorine atoms) were treated with the frozen-core approximation. The
Instantaneous interaction energy ΔE_{int} between two molecular fragments A and B in the frozen geometry of molecule AB is decomposed into three main components: $\Delta E_{int} = \Delta E_{elstat} + \Delta E_{Pauli} + \Delta E_{orb}$. The term ΔE_{elstat} corresponds to the electrostatic interaction between the unperturbed charge distributions of fragments A and B. The Pauli repulsion term ΔE_{Pauli} describes the energy change arising from the repulsive interaction caused by the Pauli exclusion principle. The orbital interaction term ΔE_{orb} is the energy gained by the relaxation of the molecular orbitals to their optimal form and accounts for charge transfer and polarization effects. The ΔE_{orb} term is further separated into contributions related to the deformation density due to the bonding with the ETS-NOCV (Natural Orbitals for Chemical Valence) scheme, computed at the same level of theory.[29] Each individual deformation density contribution, which are defined as eigenvectors that diagonalize the deformation density matrix, is associated with an eigenvalue υ_i. Complementary NOCVs with opposite eigenvalues sign can be grouped together to describe charge transfer channels between the molecular fragments. An energy contribution to the total bond energy is associated for each NOCV pair. Visualization allows the assignment of these NOCV pairs to donating and back-donating processes and identification of the participating fragment orbitals.

The topological analysis of the electron density obtained at the B3LYP/TZBP level has been done using Bader's Quantum theory of atoms in molecules (QTAIM)[19] with Multiwfn 3.6 software.[122] The bond critical points (bcp) of the C- B bond in $\mathbf{X}^{//}$-BH_2^+ and $\mathbf{X}^{\perp}$-BH_2^+ complexes have been identified and local properties (electron density ρ, ellipticipy ε, eigenvalues of $\Delta\rho$) have been compute at the bcp as well as at various positions along the B-C bond. Non-local properties (Delocalization Index DI between atomic basin of C and B atoms) have also been computed. Multiwfn software was also used

to carry out the topological analysis of the electron localization function (ELF).[20,21] This method was previously used to study the interaction between NHC and main group fragments.[123-125] It allows to determine the valence monosynaptic (lone pair) and disynaptic (bond) basins and to calculate their electronic population by integrating the electronic density on the corresponding basin. One disynaptic V(C,B) basin has been obtained for all $\mathbf{X}^{//}$-BH_2^+ and $\mathbf{X}^{\perp}$-BH_2^+ complexes except for $\mathbf{39}^{//}$-BH_2^+ for which two V(C,B) basins are presents.

The coefficient of determination R^2 has been used to compare the various computed indicators and to quantify their correlation degree. The accuracy of the predicted linear (or quadratic or logarithmic) correlation y = Ax + B for a given set of (x_i,y_i) values (i = 1 to 39) is further analysed by four numerical tests:

- The maximum error (Max), defined by Max = max | $Ax_i + B - y_i$ |
- The mean absolute deviation (MAD), obtained through MAD = [Σ_i (| $Ax_i + B - y_i$ |)]/39
- The root-mean-square deviation (RMSD) has been calculated using Equation (1)

$$\text{RMSD} = \sqrt{\frac{\sum_i (Ax_i + B - y_i)^2}{39}} \qquad (1)$$

- The normalized RMSD (NRMSD) is given by NRMSD = RMSD / [$\max_i(y_i) - \min_i(y_i)$]. NRSMD facilitates comparison between the various computed datasets and is expressed as a percentage.

Acknowledgments

This work was performed using HPC resources from GENCI-CINES (Grant A0050806894). R.G. thanks the Ecole Polytechnique for a PhD stipend. G.H. thanks the vice-presidency for marketing and international relations in Ecole Polytechnique for support from the international internship program.

Supporting Information

Descriptor's numerical values, correlation plots, deformation densities, electronic energies and Cartesian coordinates

Author information

Corresponding author

E-mail: gilles.frison@polytechnique.edu

ORCID

Radhika Gupta: 0000-0003-1562-7810
Elixabete Rezabal: 0000-0003-0397-6140
Camille Noûs: 0000-0002-0778-8115
Gilles Frison: 0000-0002-5677-3569

Notes

The authors declare no competing financial interest.

References

(1) Gonthier, J.F.; Steinmann, S.N.; Wodrich, M.D.; Corminboeuf, C. Quantification of "fuzzy" chemical concepts: a computational perspective. *Chem. Soc. Rev.* **2012**, *41*, 4671-4687.

(2) Grunenberg, J. Ill-defined chemical concepts: the problem of quantification. *Int. J. Quantum Chem.* **2017**, *117*, e25359

(3) Pauling, L. The nature of the Chemical Bond. Cornell Univ. Press, **1960**.

(4) Zhao, L.; Schwarz, W.H.; Frenking, G. The Lewis electron-pair bonding model: the physical background, one century later. *Nat. Chem. Rev.* **2019**, *3*, 35-47.

(5) Gordy, W. Dependence of bond order and of bond energy upon bond length. *J. Chem. Phys.* **1947**, *15*, 305-310.

(6) Pyykkö, P.; Atsumi, M. Molecular double-bond covalent radii for elements Li-E112. *Chem. Eur. J.* **2009**, *15*, 12770-12779.

(7) Zhao, L.; Pan, S.; Holzmann, N.; Schwerdtfeger, P.; Frenking, G. Chemical bonding and bnoding models of main-group compounds. *Chem. Rev.* **2019**, *119*, 8781-8845.

(8) Coulson, C.A. The electronic structure of some polyenes and aromatic molecules VII. Bonds of fractional order by the molecular orbital method. *Proc. R. Soc. London, Ser. A* **1939**, *169*, 413-428.

(9) Wiberg, K.B. Application of the Pople-Santry-Segal CNDO method to the cyclopropylcarbinyl and cyclobutyl cation and to bicyclobutane. *Tetrahedron* **1968**, *24*, 1083-1096.

(10) Mayer, I. charge, bond order and valence in the *ab initio* SCF theory. *Chem. Phys. Lett.* **1983**, *97*, 270-274.

(11) Mayer, I. bond order and valence indices: a personal account. *J. Comput. Chem.* **2007**, *28*, 204-221.

(12) Boys, S.F. Construction of some molecular orbitals to be approximately invariant for changes from one molecule to another. *Rev. Mod. Phys.* **1960**, *32*, 296-299.

(13) Pipek, J.; Mezey, P.G. A fast intrinsic localization procedure applicable for ab ignition and semiempirical linear combination of atomic orbital wave functions. *J. Chem. Phys.* **1989**, *90*, 4916-4926.

(14) Edmiston, C.; Ruedenberg, K. Localized atomic and molecular orbitals. *Rev. Mod. Phys.* **1963**, *35*, 457-465.

(15) Löwdin, P.O. quantum theory of many-particle systems. I. Physical interpretations by means of density matrices, natural spin-orbitals, and convergence problems in the method of configurational interaction. *Phys. Rev.* **1955**, *97*, 1474-1489.

(16) Rhee, Y.M.; Head-Gordon, M. A delicate electronic balance between metal and ligand in [Cu-P-Cu-P] Diamondoids: oxidation state dependent plasticity and the formation of a singlet diradicaloid. *J. Am. Chem. Soc.* **2008**, *130*, 3878-3887.

(17) Thom, A.J.W; Sundstrom, E.J.; Head-Gordon, M. LOBA: a localized orbital bonding analysis to calculate oxidation states, with application to a model water oxidation catalyst. *Phys. Chem. Chem. Phys.* **2009**, *11*, 11297-11304.

(18) Glendening, E.D.; Landis, C.R.; Weinhold, F. Natural Bond Orbital Methods. *WIREs Comput. Mol. Sci*. **2012**, *2*, 1-42.

(19) Bader, R.F.W. Atoms in molecules: A quantum theory. Oxford Univ. Press, **1990**.

(20) Becke, A.D.; Edgecombe, K.E. A simple measure of electron localization in atomic and molecular systems. *J. Chem. Phys.* **1990**, *92*, 5397-5403.

(21) Silvi, B.; Savin, A. Classification of chemical bonds based on topological analysis of electron localization functions. *Nature* **1994**, *371*, 683-686.

(22) Johnson, E.R.; Keinan, S.; Mori-Sanchez, P.; Contreras-Garcia, J.; Cohen, A.J.; Yang, W. Revealing noncovalent interactions. *J. Am. Chem. Soc.* **2010**, *132*, 6498-6506.

(23) de Silva, P.; Corminboeuf, C. Simultaneous visualization of covalent and noncovalent interactions using regions of density overlap. *J. Chem. Theory Comput.* **2014**, *10*, 3745-3756.

(24) Karadakov, P.B.; Horner, K.E. Exploring Chemical Bonds through Variations in Magnetic Shielding. *J. Chem. Theory Comput.* **2016**, *12*, 558-563.

(25) Bistoni, G.; Belpassi, L.; Tarantelli, F. Advances in Charge Displacement Analysis. *J. Chem. Theory Comput.* **2016**, *12*, 1236–1244.

(26) Ziegler, T.; Rauk, A. A theoretical study of the ethylene-metal bond in complexes between Cu^+, Ag^+, Au^+, Pt^0 or Pt^{2+} and ethylene, based on the Hartree-Fock-Slater transition-state method. *Inorg. Chem.* **1979**, *18*, 1558-1565.

(27) Ziegler, T.; Rauk, A. CO, CS, N_2, PF_3, and $CNCH_3$ as σ donors and π acceptors. A theoretical study by the Hartree-Fock-Slater transition-state method. *Inorg. Chem.* **1979**, *18*, 1755-1759.

(28) Morokuma, K. Molecular orbital studies of hydrogen bonds. III. C=O···H-O hydrogen bond in $H_2CO{\cdots}H_2O$ and $H_2CO{\cdots}2H_2O$. *J. Chem. Phys.* **1971**, *55*, 1236-1244.

(29) Mitoraj, M.P.; Michalak, A.; Ziegler, T. A combined charge and energy decomposition scheme for bond analysis. *J. Chem. Theory Comput.* **2009**, *5*, 962-975.

(30) Jeziorski, B.; Moszynski, R.; Szalewicz, K. Perturbation theory approach to intermolecular potential energy surfaces of van der Waals complexes. *Chem. Rev.* **1994**, *94*, 1887-1930.

(31) Kaupp, M.; Danovich, D.; Shaik, S. Chemistry is about energy and its changes: A critique of bond-length/bond-strength correlations. *Coord. Chem. Rev.* **2017**, *344*, 355-362.

(32) Kraka, E.; Cremer, D. Characterization of CF bonds with multiple-bond character: bond lengths, stretching force constants, and bond dissociation energies. *ChemPhysChem* **2009**, *10*, 686-698.

(33) Setiawan, D.; Kalescky, R.; Kraka, E.; Cremer, D. Direct measure of metal-ligand bonding replacing the Tolman electronic parameter. *Inorg. Chem.* **2016**, *55*, 2332-2344.

(34) Brandhorst, K.; Grunenberg, J. How strong is it? The interpretation of force and compliance constants as bond strength descriptors. *Chem. Soc. Rev.* **2008**, *37*, 1558-1567.

(35) Zhao, L.; Hermann, M.; Schwarz, W.H.E.; Frenking, G. The Lewis electron-pair bonding model: modern energy decomposition analysis. *Nat. Rev. Chem.* **2019**, *3*, 48-63.

(36) Pecher, L.; Tonner, R. Deriving bonding concepts for molecules, surfaces, and solids with energy decomposition analysis for extended systems. *WIREs Comput. Mol. Sci.* **2019**, *9*, e1401.

(37) Zhao, L.; von Hopffgarten, M.; Andrada, D.M.; Frenking, G. Energy decomposition analysis. *WIREs Comput. Mol. Sci.* **2018**, *8*, e1345.

(38) Lepetit, C.; Fau, P.; Fajerwerg, K.; Kahn, M.L.; Silvi, B. Topological analysis of the metal-metal bond: a tutorial review. *Coord. Chem. Rev*. **2017**, *345*, 150-181.

(39) Weinhold, F.; Landis, C.R.; Glendening, E.D. What is NBO analysis and how is it useful? *Int. Rev. Phys. Chem.* **2016**, *35*, 399-440.

(40) Dognon, J.P. Theoretical insights into the chemical bonding in actinide complexes. *Coord. Chem. Rev.* **2014**, 266-267, 110-122.

(41) Matito, E.; Sola, M. The role of electronic delocalization in transition metal complexes from the electron localization function and the quantum theory of atoms in molecules viewpoints. *Coord. Chem. Rev.* **2009**, *253*, 647-665.

(42) Bader, R.F.W. A quantum theory of molecular structure and its applications. *Chem. Rev.* **1991**, *91*, 893-928.

(43) Dutta, S.; Maity, B.; Thirumalai, D.; Koley, D. Computational investigation of carbene-phosphinidenes : correlation between 31P chemical shifts and bonding features to estimate the pi-backdonation of carbenes. *Inorg. Chem.* **2018**, *57*, 3993-4008.

(44) Cortes-Guzman, F.; Bader, R.F.W. Complementarity of QTAIM and MO theory in the study of bonding in donor-acceptor complexes. *Coord. Chem. Rev.* **2005**, *249*, 633-662.

(45) Fugel, M.; Beckmann, J.; Jayatilaka, D.; Gibbs, G.V.; Grabowsky, S. A variety of bond analysis methods, one answer? An investigation of the element-oxygen bond of hydroxides H_nXOH. *Chem. Eur. J.* **2018**, *24*, 6248-6261.

(46) Fugel, M.; Hesse, M.F.; Pal, R.; Beckmann, J.; Jayatilaka, D.; Turner, M.J.; Karton, A.; Bultinck, P.; Chandler, G.S.; Grabowsky, S. Covalency and iconicity do not oppose each other – relationship between Si-O bond character and basicity of siloxanes. *Chem. Eur. J.* **2018**, *24*, 15275-15286.

(47) Wu, X.; Zhao, L.; Jin, J.; Pan, S.; Li, W.; Jin, X.; Wang, G.; Zhou, M.; Frenking, G. Observation of alkaline earth complexes M(CO)8 (M = Ca, Sr, or Ba) that mimic transition metals. *Science*, **2018**, *361*, 912-916.

(48) Landis, C.R.; Hughes, R.P.; Weinhold, F. Comment on "Observation of alkaline earth complexes M(CO)8 (M = Ca, Sr, or Ba) that mimic transition metals". *Science*, **2019**, *365*, 10.1126/science.aay2355.

(49) Zhao, L.; Pan, S.; Zhou, M.; Frenking, G. Response to Comment on "Observation of alkaline earth complexes M(CO)8 (M = Ca, Sr, or Ba) that mimic transition metals". *Science*, **2019**, *365*, 10.1126/science.aay5021.

(50) Landis, C.R.; Hughes, R.P.; Weinhold, F. Bonding Analysis of $TM(cAAC)_2$ (TM = Cu, Ag, and Au) and the Importance of Reference State. *Organometallics*, **2015**, *34*, 3442–3449

(51) Jerabek, P.; Roesky, H.W.; Bertrand, G.; Frenking, G. Coinage Metals Binding as Main Group Elements: Structure and Bonding of the Carbene Complexes $[TM(cAAC)_2]$ and $[TM(cAAC)_2]^+$ (TM = Cu, Ag, Au). *J. Am. Chem. Soc.* **2014**, *136*, 17123-17135.

(52) Molina Molina, J.; Dobado, J.A.; Heard, G.L.; Bader, R.F.W.; Sundberg, M.R. Recognizing a triple bond between main group atoms. *Theor. Chem. Acc.* **2001**, *105*, 365-373.

(53) Xie, Y.; Grev, R.S.; Gu, J.; Schaefer III, H.F.; Schleyer, P.v.R.; Su, J.; Li, X.W.; Robinson, G.H. The nature of the gallium-gallium triple bond. *J. Am. Chem. Soc.* **1998**, *120*, 3773-3780.

(54) Klinkhammer, K.W. How can one recognize a triple bond between main group elements. *Angew. Chem. Int. Ed. Engl.* **1997**, *36*, 2320-2322.

(55) Weinhold, F.; Klein, R.A. Improved general understanding of the hydrogen-bonding phenomena: A reply. *Angew. Chem. Int. Ed.* **2015**, *54*, 2600-2602.

(56) Frenking, G.; Caramori, G.F. No need for a re-examination of the electrostatic notation of the hydrogen bonding: A comment. *Angew. Chem. Int. Ed.* **2015**, *54*, 2596-2599.

(57) Weinhold, F.; Klein, R.A. Anti-electrostatic hydrogen bonds. *Angew. Chem. Int. Ed.* **2014**, *53*, 11214-11217.

(58) Stone, A.J.; Szalewicz, K. Reply to "Comment on « Natural bond orbitals and the nature of the hydrogen bond »". *J. Phys. Chem. A* **2018**, *122*, 733-736.

(59) Weinhold, F.; Glendening, E.D. Comment on « Natural bond orbitals and the nature of the hydrogen bond ». *J. Phys. Chem. A* **2018**, *122*, 724-732.

(60) Stone, A.J. Natural bond orbitals and the nature of the hydrogen bond. *J. Phys. Chem. A* **2017**, *121*, 1531-1534.

(61) Weinhold, F.; von Ragué Schleyer, P.; McKee, W.C. Bay-type H···H "bonding" in cis-2-butene and related species: QTAIM versus NBO description. *J. Comput. Chem.* **2014**, *35*, 1499-1508.

(62) Bickelhaupt, F.M.; Baerends, E.J. The case for steric repulsion causing the staggered conformation of ethane. *Angew. Chem. Int. Ed.* **2003**, *42*, 4183-4188.

(63) Weinhold, F. Rebuttal to the Bickelhaupt-Baerends case for steric repulsion causing the staggered conformation of ethane. *Angew. Chem. Int. Ed.* **2003**, *42*, 4188-4194.

(64) Andrada, D.M.; Holzmann, N.; Hamadi, T.; Frenking, G. Direct estimate of the internal π-donation to the carbene centre within N-heterocyclic carbenes and related molecules. *Beilstein J. Org. Chem.* **2015**, *11*, 2727-2736.

(65) Ayers, P.L.; Boyd, R.J.; Bultinck, P.; Caffarel, M.; Carbo-Dorca, R.; Causa, M.; Cioslowski, J.; Contreras-Garcia, J.; Cooper, D.L.; Coppens, P.; Gatti, C.; Grabowsky, S.; Lazzeretti, P.; Macchi, P.; Martin Pendas, A.; Popelier, P.L.A.; Ruedenberg, K.; Rzepa, H.; Savin, A.; Sax, A.; Schwarz, W.H.E.; Shahbazian, S.; Silvi, B.; Sola, M.; Tsirelson, V. Six questions on topology in theoretical chemistry. *Comput. Theor. Chem.* **2015**, *1053*, 2-16.

(66) Andrés, J. ; Ayers, P.W.; Boto, R.A.; Carbo-Dorca, R.; Chermette, H.; Cioslowski, J.; Contreras-Garcia, J.; Cooper, D.L.; Frenking, G.; Gatti, C.; Heidar-Zadeh, F.; Joubert, L.; Martin Pendas, A.; Matito, E.; Mayer, I.; Misquitta, A.J.; Mo, Y.; Pilmé, J.; Popelier, P.L.A.; Rahm, M.; Ramos-Cordobo, E.; Salvador, P.; Schwarz, W.H.E.; Shahbazian, S.; Silvi, B.; Sola, M.; Szalewicz, K.; Tognetti, V.; Weinhold, F.; Zinc, E.L. Nine questions on energy decomposition analysis. *J. Comput. Chem.* **2019**, *40*, 2248-2283.

(67) Weinhold, F. Natural bond orbital analysis: a critical overview of relationships to alternative bonding perspectives. *J. Comput. Chem.* **2012**, *33*, 2363-2379.

(68) Weinhold, F. Natural bond critical point analysis: quantitative relationships between natural bond orbital-based and QTAIM-based topological descriptors of chemical bonding. *J. Comput. Chem.* **2012**, *33*, 2440-2449.

(69) Sola, M. Why aromaticity is a suspicious concept ? Why ? *Front. Chem.* **2017**, *5*, 22.

(70) Sola, M. Connecting and combining rules of aromaticity. Towards a unified theory of aromaticity. *WIREs Comput. Mol. Sci.* **2019**, *9*, e1404.

(71) Piers, W.E.; Bourke, S.C.; Conroy, K.D. Borinium, borenium, and boronium ions: synthesis, reactivity, and applications. *Angew. Chem. Int. Ed.* **2005**, *44*, 5016-5036.

(72) Farrell, J.M.; Hatnean, J.A.; Stephan, D.W. Activation of hydrogen and hydrogenation catalysis by a borenium cation. *J. Am. Chem. Soc.* **2012**, *134*, 15728-15731.

(73) De Vries, T.S.; Prokofjevs, A.; Vedejs, E. Cationic tricoordinate boron intermediates: borenium chemistry from the organic perspective. *Chem. Rev.* **2012**, *112*, 4246-4282.

(74) Eisenberger, P.; Crudden, C.M. Borocation catalysis. *Dalton. Trans.* **2017**, *46*, 4874-4887.

(75) Rao, B.; Kinjo, K. Boron-based catalysts for C-C bond-formation reactions. *Chem. Asian J.* **2018**, *13*, 1279-1292.

(76) Ingleson, M.J. Fundamental and applied properties of borocations. *Top. Organomet. Chem.* **2015**, *49*, 39-71.

(77) Franz, D.; Inoue, S. Cationic complexes of boron and aluminium : an early 21st century viewpoint. *Chem. Eur. J.* **2019**, *25*, 2898-2926.

(78) Fustier-Boutignon, M.; Nebra, N.; Mézailles, N. Geminal dianions stabilized by main group elements. *Chem. Rev.* **2019**, *119*, 8555-8700.

(79) Radcliffe, J.E.; Dunsford, J.J.; Cid, J.; Fasano, V.; Ingleson, M.J. N-heterocycle-ligated borocations as highly tunable carbon Lewis acids. *Organometallics*, **2017**, *36*, 4952-4960.

(80) Matsumoto, T.; Gabbaï, F. A borenium cation stabilized by an N-heterocyclic carbene ligand. *Organometallics* **2009**, *28*, 4252-4253.

(81) McArthur, D.; Butts, C.P.; Lindsay, D.M. A dialkylborenium ion *via* reaction of *N*-heterocyclic carbene-organoboranes with Bronsted acids-synthesis and DOSY NMR studies. *Chem. Commun.* **2011**, *47*, 6650-6652.

(82) Mansaray, H.B.; Rowe, A.D.L.; Phillips, N.; Niemeyer, J.; Kelly, M.; Addy, D.A.; Bates, J.I.; Aldridge, S. Modelling fundamental arene-borane contacts: spontaneous formation of a dibromoborenium cation driven by interaction between a borane Lewis acid and an arene π system. *Chem. Commun.* **2011**, *47*, 12295-12297.

(83) Prokofjevs, A.; Boussonière, A.; Li, L.; Bonin, H.; Lacôte, E.; Curran, D.P.; Vedejs, E. Borenium ion catalyzed hydroboration of alkenes with N-heterocyclic carbene-boranes. *J. Am. Chem. Soc.* **2012**, *134*, 12281-12288.

(84) Tay, M.Q.Y.; Murugesapandian, B.; Lu, Y.; Ganguly, R.; Rei, K.; Vidovic, D. Dihaloborenium cations stabilized by a four-membered N-heterocyclic carbene: electron deficiency compensation by asymmetric structural changes. *Dalton Trans.* **2014**, *43*, 15313-15316.

(85) Farrell, J.M. ; Schmidt, D.; Grande, V.; Würthner, F. Synthesis of a doubly boron-doped perylene through NHC-borenium hydroboration/C-H borylation/dehydrogenation. *Angew. Chem. Int. Ed.* **2017**, *56*, 11846-11850.

(86) Eisenberger, P.; Bestvater, B.P. ; Keske, E.C. ; Crudden, C.M. Hydrogenation at room temperature and atmospheric pressure with mesoionic carbene-stabilized borenium catalysts. *Angew. Chem. Int. Ed.* **2015**, *54*, 2467-2471.

(87) Münzer, J.E.; Ona-Burgos, P.; Arrabal-Campos, F.M.; Neumüller, B.; Tonner, R.; Fernandez, I.; Kuzu, I. Difluoroborenium cation stabilized by hexaphenyl-carbodiphosphorane: a concise study on the molecular and electronic structure of $[(Ph_3P)_2C\rightarrow BF_2][BF_4]$. *Eur. J. Inorg. Chem.* **2016**, 3852-3858.

(88) Inés, B.; Patil, M.; Carreras, J.; Goddard, R.; Thiel, W.; Alcarazo, M. Synthesis, structure, and reactivity of a dihydrido borenium cation. *Angew. Chem. Int. Ed.* **2011**, *50*, 8400-8403.

(89) Lafage, M.; Pujol, A.; Saffon-Merceron, N.; Mézailles, N. BH3 activation by phosphorus-stabilized geminal dianions: synthesis of ambiphilic organoborane, DFT studies, and catalytic CO_2 reduction into methanol derivatives. *ACS Catal.* **2016**, *6*, 3030-3035.

(90) Celik, M.A.; Frenking, G.; Neumüller, B.; Petz, W. Exploiting the twofold donor ability of carbodiphosphoranes: theoretical studies of $[(Ph_3P)_2C\rightarrow EH_2]^q$ (E^q = Be, B^+, C^{2+}, N^{3+}, O^{4+}) and synthesis of the dication $[(Ph_3P)_2C{=}CH_2]^{2+}$. *ChemPlusChem* **2013**, *78*, 1024-1032.

(91) Frenking, G.; Hermann, M.; Andrada, D.M.; Holzmann, N. Donor-acceptor bonding in novel low-coordinated compounds of boron and groupe-14 atoms C-Sn. *Chem. Soc. Rev.* **2016**, *45*, 1129-1144.

(92) Nhung, N.T.A.; Loan, H.T.P.; Son, P.T.; Duc, H.V.; Quang, D.T.; Tat, P.V.; Hlep, D.T. Theoretical assessment of donor-acceptor complexes $[X(PPh_3)_2 \rightarrow AlH_2]^+$ (X=C-Pb): structures and bonding. *Theor. Chem. Acc*. **2019**, *138*, 67.

(93) Sato, K.; Tsai Yuan Tan, T.; Schäfers, F.; Hahn, F.E.; Stephan, D.W. Imidazole-stabilized, electron-deficient boron cations. *Dalton. Trans.* **2017**, *46*, 16404-16407.

(94) Tsai, H.C.; Lin, Y.F.; Liu, W.C.; Lee, G.H.; Peng, S.M.; Chiu, C.W. N-heterocyclic silylene coordinated dialkyl borenium equivalent. *Organometallics*, **2017**, *36*, 3879-3882.

(95) Rezabal, E.; Frison, G. Estimating π binding energy of N-heterocyclic carbenes: the role of polarization. *J. Comput. Chem.* **2015**, *36*, 564-572.

(96) Huynh, H.V.; Frison, G. Electronic structural trends in divalent carbon compounds. *J. Org. Chem.* **2013**, *78*, 328-338.

(97) Bernhammer, J.C.; Frison, G.; Huynh, H.V. Electronic structure trends in N-heterocyclic carbenes (NHCs) with varying number of nitrogen atoms and NHC-transition-metal bond properties. *Chem. Eur. J.* **2013**, *19*, 12892-12905.

(98) Huynh, H.V. Electronic properties of N-heterocyclic carbenes and their experimental determination. *Chem. Rev.* **2018**, *118*, 9457-9492.

(99) Munz, D. Pushing electrons – which carbene ligand for which application? *Organometallics* **2018**, *37*, 275-289.

(100) The largest deviation is observed for **8**-BH_2^+ with Y-C-B-H dihedral angle of 13.8°, due to the non-planarity of the NHC moiety.

(101) WBI values have also been calculated for **X**-BH_3 complexes, and the use of these values leads to similar analyses to the ones obtained with WBI(**X**$^{\perp}$-BH_2^+).

(102) Rogachev, A.Y.; Hoffmann, R. Hypervalent compounds as ligands: I3-anion adducts with transition metal pentacarbonyls. *Inorg. Chem.* **2013**, *52*, 7161-7171.

(103) Bader, R.F.W.; Tang, T.H.; Tal, Y.; Biegler-König, F.W. Properties of atoms and bonds in hydrocarbon molecules. *J. Am. Chem. Soc.* **1982**, *104*, 946-952.

(104) Matta, C.F.; Hernandez-Trujillo, J. Bonding in polycyclic aromatic hydrocarbons in terms of the electron density and of electron delocalization. *J. Phys. Chem. A* **2003**, *107*, 7496-7504.

(105) Outeiral, C.; Vincent, M.A.; Martin Pendas, A.; Popelier, P.L.A. Revitalizing the concept of bond order through delocalization measures in real space. *Chem. Sci.* **2018**, *9*, 5517-5529.

(106) Bader, R.F.W.; Slee, T.S.; Cremer, D.; Kraka, E. Description of conjugation and hyperconjugation in terms of electron distributions. *J. Am. Chem. Soc.* **1983**, *105*, 5061-5068.

(107) Frisch, M. J.; Trucks, G. W.; Schlegel, H. B.; Scuseria, G. E.; Robb, M. A.; Cheeseman, J. R.; Scalmani, G.; Barone, V.; Mennucci, B.; Petersson, G. A.; Nakatsuji, H.; Caricato, M.; Li, X.; Hratchian, H. P.; Izmaylov, A. F.; Bloino, J.; Zheng, G.; Sonnenberg, J. L.; Hada, M.; Ehara, M.; Toyota, K.; Fukuda, R.; Hasegawa, J.; Ishida, M.; Nakajima, T.; Honda, Y.; Kitao, O.; Nakai, H.; Vreven, T.; Montgomery, J. A. Jr.; Peralta, J. E.; Ogliaro, F.; Bearpark, M.; Heyd, J. J.; Brothers, E.; Kudin, K. N.; Staroverov, V. N.; Kobayashi, R.; Normand, J.; Raghavachari, K.; Rendell, A.; Burant, J. C.; Iyengar, S. S.; Tomasi, J.; Cossi, M.; Rega, N.; Millam, J. M.; Klene, M.; Knox, J. E.; Cross, J. B.; Bakken, V.; Adamo, C.; Jaramillo, J.; Gomperts, R.; Stratmann, R. E.; Yazyev, O.; Austin, A. J.; Cammi, R.; Pomelli, C.; Ochterski, J. W.; Martin, R. L.; Morokuma, K.; Zakrzewski, V. G.; Voth, G. A.; Salvador, P.; Dannenberg, J. J.; Dapprich, S.; Daniels, A. D.; Farkas, Ö.; Foresman, J. B.; Ortiz, J. V.; Cioslowski, J.; Fox, D. J. Gaussian, Inc., Wallingford CT, Gaussian 09, Revision D.01, **2013**.

(108) Becke, A.D. Density-functional exchange-energy approximation with correct asymptotic-behavior. *Phys. Rev. A* **1988**, *38*, 3098-3100.

(109) Lee, C.; Yang, W.; Parr, R.G. Development of the Colle-Salvetti correlation-energy formula into a functional of the electron density. *Phys. Rev. B* **1988**, *37*, 785-789.

(110) Schaefer, A.; Horn, H.; Ahlrichs, R. Fully optimized contracted Gaussian-basis sets for atoms Li to Kr. *J. Chem. Phys.* **1992**, *97*, 2571-2577.

(111) Schaefer, A.; Huber, C.; Ahlrichs, R. Fully optimized contracted Gaussian-basis sets of triple zeta valence quality for atoms Li to Kr. *J. Chem. Phys.* **1994**, *100*, 5829-5835.

(112) Zhao, Y.; Truhlar, D.G. The M06 suite of density functionals for main group thermochemistry, thermochemical kinetics, noncovalent interactions, excited states, and transition elements: two new functionals and systematic testing of four M06-class functionals and 12 other functionals. *Theor. Chem. Acc.* **2008**, *120*, 215-241.

(113) McLean, A.D.; Chandler, G.S. Contracted Gaussian-basis sets for molecular calculations. 1. 2nd row atoms, Z=11-18. *J. Chem. Phys.* **1980**, *72*, 5639-5648.

(114) Raghavachari, K.; Binkley, J.S.; Seeger, R.; Pople, J.A. Self-Consistent Molecular Orbital Methods. XX. Basis set for correlated wave-functions. *J. Chem. Phys.* 1980, **72**, 650-654.

(115) Glendening, E.D.; Badenhoop, J.K.; Reed, A.E.; Carpenter, J.E.; Bohmann, J.A.; Morales, C.M.; Landis, C.R.; Weinhold, F. NBO 6.0; Theoretical Chemistry Institute, University of Wisconsin, Madison, WI, **2013**.

(116) Glendening, E.D.; Landis, C.R.; Weinhold, F. NBO 6.0: Natural bond orbital analysis program. *J. Comput. Chem.* **2013**, *34*, 1429-1437.

(117) Tay, M.Q.Y.; Ilic, G.; Werner-Zwanziger, U.; Lu, Y.; Ganguly, R.; Ricard, L.; Frison, G.; Carmichael, D.; Vidovic, D. Preparation, structural analysis and reactivity studies of phosphenium dications. *Organometallics* **2016**, *35*, 439-449.

(118) Fonseca Guerra, C.; Snijders, J.G. ; Te Velde, G. ; Baerends, E.J. Towards an order-N DFT method. *Theor. Chem. Acc.* **1998**, *99*, 391-403.

(119) Te Velde, G. ; Bickelhaupt, F.M. ; Baerends, E.J. ; Fonseca Guerra, C. ; Van Gisbergen, S.J.A. ; Snijders, J.G. ; Ziegler, T. Chemistry with ADF. *J. Comput. Chem.* **2001**, *22*, 931-967.

(120) *ADF2017*, SCM, Theoretical Chemistry, Vrije Universiteit, Amsterdam, The Netherlands, http://www.scm.com.

(121) Van Lenthe, E. ; Baerends, E.J. Optimized Slater-type basis sets for the elements 1–118. *J. Comput. Chem.* **2003**, *24*, 1142-1156.

(122) Lu, T.; Chen, F. Multiwfn: A Multifunctional Wavefunction Analyzer, *J. Comp. Chem.* **2012**, *33*, 580-592.

(123) Frison, G.; Sevin, A. A DFT/Electron Localization Function (ELF) study of the bonding of phosphinidenes with N-heterocyclic carbenes. *J. Phys. Chem. A* **1999**, *103*, 10998-11003.

(124) Frison, G.; Sevin, A. Substituent effects in polarized phosphaalkenes : a theoretical study of aminocarbene-phosphinidene adducts. *J. Organomet. Chem*. **2002**, *643-644*, 105-111.

(125) Frison, G.; Sevin, A. Theoretical study of the bonding between aminocarbene and main group elements. *J. Chem. Soc., Perkin Trans. 2* **2002**, 1692-1697.

TOC/Abstract Graphic